PHYSICAL REVIEW B VOLUME 50, NUMBER 6 1 AUGUST 1994-II

Dependence of giant magnetoresistance on grain size in Co/Cu multilayers

A. R. Modak and David J. Smith*
Center for Solid State Science, Arizona State University, Tempe, Arizona 85287

S. S. P. Parkin
IBM Research Division, Almaden Research Center, 650 Harry Road, San Jose, California 95120-6099

(Received 9 May 1994)

The effect of grain size on the magnetoresistance (MR) of Co/Cu multilayers fabricated by dc magnetron sputtering has been studied using Co/Cu multilayers grown with identical Co and Cu thicknesses but different grain sizes. These multilayers were selectively fabricated by growing with and without a Cu underlayer: grain-to-grain epitaxy from the buffer layer to the superlattice in the former facilitated control of the multilayer grain structure. The MR was found to increase with increasing grain size, with the difference being larger at low temperature. The enhancement of MR is attributed to an increased electron mean free path leading to sampling of more antiferromagnetically coupled layers.

Metallic multilayers comprised of alternating magnetic and nonmagnetic layers exhibit oscillatory interlayer magnetic exchange coupling[1–5] and giant magnetoresistance (GMR) when the magnetic layers are coupled antiferromagnetically.[1–8] When a high magnetic field (saturation field) is applied to a multilayer with antiferromagnetically coupled layers, there is a change in the magnetic structure (from antiparallel to parallel arrangement of magnetic layers) which gives rise to the observed change in electrical resistivity. The saturation magnetoresistance (MR) is usually defined as a percentage: it is the difference between the peak resistivity and the resistivity at saturation field divided by the high field resistivity. Many combinations of magnetic metals and alloys (e.g., Fe, Co, NiFe), and transition and noble metal spacers (e.g., Cu, Ru, V, Mo, Ag) exhibit GMR and coupling.[1,3,4] Co/Cu multilayers show the greatest room temperature MR so far reported and they continue to be extensively investigated.[2,3,9–16] The room temperature MR values in this system exceed 65%, for the first peak, with values as high as 120% at 4.2 K.[9]

The first demonstration of GMR properties utilized epitaxial multilayers fabricated by molecular beam epitaxy[1,2] but enormous progress has since been made using multilayers deposited by simpler techniques such as magnetron sputtering[1,3,4,9] and evaporation.[2,6] A key feature of thin films deposited using these latter techniques is their polycrystalline structure. Their polycrystallinity prompts immediate questions about the influence of grain size, morphology, orientation, and texture on the magnetoresistive response. For example, grain boundary scattering is likely to influence resistivity of a thin film. Additionally, grain boundaries are a form of structural disorder and they may also have indirect structure-related effects on MR. Boundaries running parallel to the layers may affect layer and/or interface roughness thus influencing interlayer coupling as well as MR. The crystallographic orientation of the bilayer in the direction of periodicity may influence the magnetic coupling strength as well as the oscillation period for transition from the antiferromagnetic to ferromagnetic state.[12,17,18] Hence, individual grain orientation and texture in the polycrystalline matrix are likely to be important in influencing the magnetoresistive response.[12] The influence of interface roughness on MR and interlayer coupling is not completely understood because of experimental difficulties in both systematically tailoring roughness and characterizing it at the atomic level. These various microstructural effects must be fully understood and taken into account when trying to correlate any nominal structure with the corresponding magnetoresistive behavior.

Co/Cu multilayers with different Cu spacer thicknesses have been investigated using high-resolution transmission electron microscopy.[10,19] They had a predominantly columnar structure with grain sizes of several bilayer periods, also increasing with Cu spacer thickness. In multilayers with relatively thick Cu spacers (85–350 Å), large grains were observed that spanned at least 3–4 bilayers. Multilayers with 350 Å Cu spacers had grains up to 5000–6000 Å wide, extending through the entire multilayer. However, multilayers with thin Cu layers (10–40 Å), of primary importance because of their large MR values, had a fine grain structure. For example, the typical grain size was in the range of 40–60 Å for the multilayer having nominal 10 Å Co and 10 Å Cu layers. This fine grain morphology cannot be neglected in consideration of resistive phenomena since the grain size could limit the effective mean free path for electron scattering. The issue of grain size can only be resolved by studying the Co/Cu multilayers with identical nominal structures (thicknesses of Co and Cu and number of bilayers) but distinctly different grain sizes. In this paper we address this question of grain size by fabricating suitable structures and studying their magnetoresistance properties.

Established approaches for changing the grain size in sputtered thin films include varying sputtering pressure, deposition rates or substrate temperature.[20–22] These techniques are useful for thin films of pure metals or alloys but in multilayers with thin Co and Cu layers, interdiffusion of individual layers may also occur leading to reduction or elimination of any GMR. For the same reason, *ex situ* heating must be excluded. The grain size differences must therefore be imparted during the growth process itself. We have de-

0163-1829/94/50(6)/4232(4)/$06.00

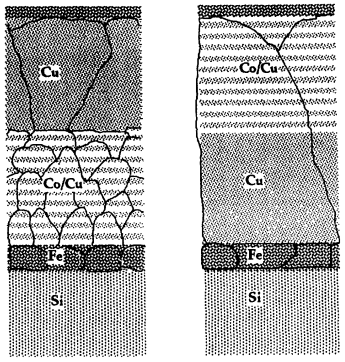

FIG. 1. Schematic illustration of proposed nominal multilayer structures and expected grain sizes.

vised an approach that utilizes grain-to-grain expitaxy[20,23] to induce large grain growth in the multilayers.

A common observation in sputtered and evaporated thin films, rather than multilayers, especially for low-melting-point metals and alloys, is that the grain size is on the same order as the film thickness. For example, this was observed in Ni-Fe, Ni-Co thin films (100–1000 Å) (Refs. 24 and 25) as well as Al films in a relatively thick film regime (1000–10 000 Å).[26] Additionally, since grain size is limited to about 2 to 3 times the film thickness due to grain growth stagnation,[27] the final thickness should determine the final grain size assuming that the atoms had substantial mobility during growth. Sputtered species have high kinetic energy and surface mobility[20,28] allowing rearrangements in structure during film growth. It follows that a thin film of a single metal should have a grain size on the same order as its thickness.

The approach we have adopted is to deposit two Co/Cu multilayers of identical nominal structure; one directly on the substrate and another on a thick Cu underlayer (350 Å). The 350 Å Cu layer is expected to have large grains (~350 Å) that would propagate into the multilayer by grain-to-grain expitaxy. The second multilayer, grown directly on the substrate, is already known from previous studies to have fine-grain morphology.[19] However, the effective resistivity of a structure with an underlayer includes resistivity intrinsic to the multilayer as well as a shunting resistivity component due to the thick Cu underlayer. To compensate for its contribution, a 350-Å thick Cu overlayer was grown on top of the multilayer stack for the second structure. In effect, we would thus obtain the desired multilayers with different grain sizes having magnetoresistive properties that can be directly compared and interpreted in relation to their intrinsic structural differences. A schematic of the nominal structures and the expected grain sizes is shown in Fig. 1.

The multilayers in this study were fabricated in a computer controlled dc magnetron sputtering system that had a base pressure of 2×10^{-9} Torr. The depositions were carried out with an approximate deposition rate of 2 Å/sec, in 3.3 mTorr of Ar^+, with the substrate held at ~40 °C. It was found earlier[9] that use of an Fe buffer layer led to flat Co and Cu layers, giving the best GMR properties. Hence, the multilayers were deposited on Si(100) wafers that had first been coated with 50 Å Fe buffer layers. The MR measurements were made with a low frequency ac four-point probe in-line technique with magnetic field, in-plane, applied either perpendicular or parallel to the current. Details of the measurement technique can be found elsewhere.[10]

Specimens for transmission electron microscopy were prepared by a standard method[29] involving cross sectioning followed by mechanical polishing, dimpling, and final thinning by Ar^+ ion milling (~4.5 kV, 1 mA) using a liquid nitrogen stage. The samples were cross sectioned such that the direction of observation would be parallel to the substrate surface and along the [110] zone axis. All observations were made with a JEM-4000EX high resolution transmission electron microscope operated at 400 kV (point-to-point resolution ~1.7 Å). A double-tilt specimen holder was used to orient samples with the incident beam aligned parallel to the Si[110] zone axis and perpendicular to the substrate normal. The microstructure could thus be studied as a function of distance from the substrate. Diffraction contrast and defocussing techniques[19,30,31] were used to obtain compositional contrast from the multilayers. Selected area electron diffraction (SAED) was used to study the presence of texturing and long-range orientational relationships.

Figure 2 shows transmission electron micrographs and a SAED pattern from the multilayer with a nominal structure Si(100)/Fe(50 Å)/{Co(10 Å)/Cu(20 Å)}$_{15}$/Co(10 Å)/Cu(350 Å)/Fe(25 Å). Figures 2(a) and 2(b) were recorded at optimum defocus and large underfocus, respectively. The successive layers of native oxide, Fe buffer layer, Co/Cu multilayer, and Cu overlayer can be distinguished. The Cu layer clearly has a large grain structure (different grains are demarcated as regions of different intensity due to diffraction contrast) with the grain size being on the order of the capping layer thickness (350 Å). The multilayer has a fine grain structure which is clear from the array of Moire fringes visible in the matrix. This structure is clearer in the higher magnification micrograph shown in Fig. 2(c). The compositional contrast is only faintly visible but the atomic structure is distinct. In some multilayer regions, individual grains can be seen while other areas show groups of Moire fringes caused by overlapping small grains. From a series of images taken along the multilayer, the average grain size was estimated to be in the range of 100–200 Å.

Compositional contrast from the multilayer can be accentuated by using a small objective aperture and defocussing the objective lens. The enhancement of contrast obvious in Fig. 2(b) results from an increase in scattering factor contrast from the different elements due to defocussing as well as delineation of interfaces due to Fresnel fringes.[32] The individual Co and Cu layers can be distinguished and are seen to be smooth and continuous, and without obvious interlayer bridging. The inset to Fig. 2(c) shows the selected area electron diffraction (SAED) pattern recorded from this sample. The major spots correspond to the Si substrate oriented in the [110] zone axis. Several grains from the polycrystalline Co/Cu superlattice are included inside the selected area aperture giving rise to a ring of spots, with the first ring corresponding to the Co/Cu (111) spacing. No predominant texturing effects are evident here although similar multilayers, investigated previously, showed a preferred (111) normal orientation.

Figure 3 shows transmission electron micrographs taken from the multilayer with the nominal structure Si(100)/Fe(50

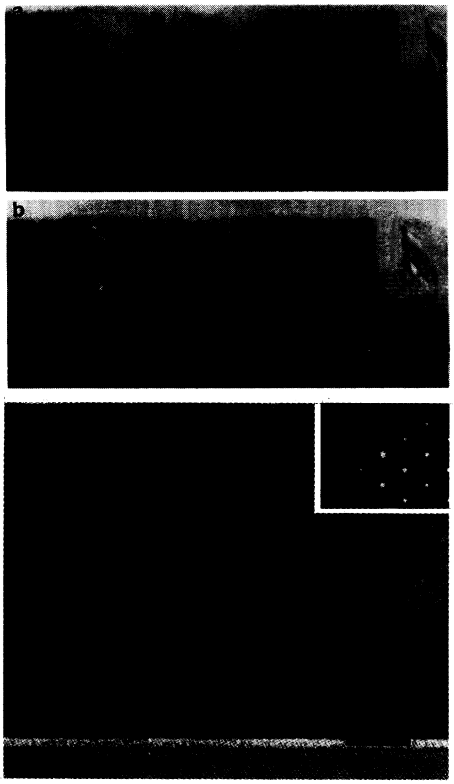

FIG. 2. (a) Bright-field transmission electron micrograph showing cross section of Co/Cu multilayer with nominal structure Si(100)/Fe(50 Å)/{Co(10 Å)/Cu(20 Å)}$_{15}$/Co(10 Å)/Cu(350 Å)/Fe(25 Å). (b) Image at large underfocus (~2000 Å) showing compositional layering. (c) High resolution electron micrograph showing characteristic fine grain structure. SAED pattern (inset) shows [110] oriented Si(100) spots and Co/Cu diffraction rings.

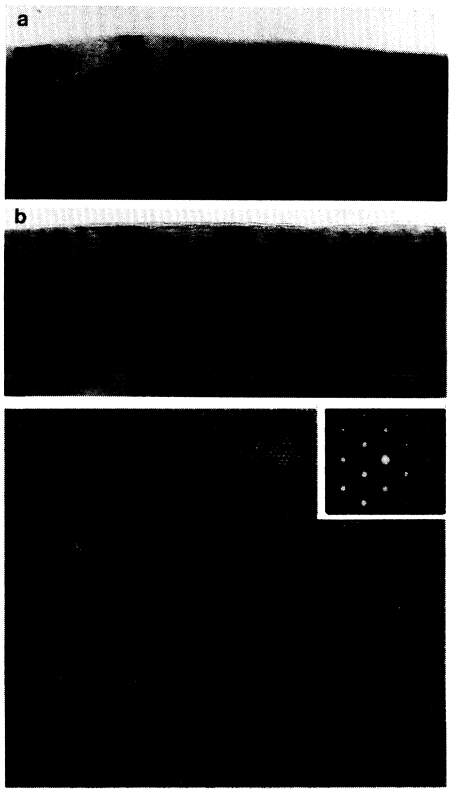

FIG. 3. (a) Bright field transmission electron micrographs showing cross section of Co/Cu multilayer with nominal structure Si(100)/Fe(50 Å)/Cu(350 Å)/{Co(10 Å)/Cu(20 Å}$_{15}$/Co(10 Å)/Fe(25 Å). (b) Image at large underfocus (~2000 Å) from same multilayer showing compositional layering. (c) High resolution electron micrograph showing grain-to-grain epitaxy at Cu/{Co/Cu} interface (marked by an arrow). Cu(111) planes are visible extending through Cu as well as {Co/Cu} superlattice.

Å)/Cu(350 Å)/{Co(10 Å)/Cu(20 Å)}$_{15}$/Co(10 Å)/Fe(25 Å). Figures 3(a) and 3(b) show images recorded at optimum defocus and large underfocus, respectively. The Cu underlayer has large grains, with an average size ~350 Å, that are columnar and extend through its entire thickness. The underlayer grain structure has clearly influenced the growth of the multilayer since large grains extend through the entire 15 biperiods in most cases, although occasional small grains are visible randomly scattered in the matrix. The grain-to-grain epitaxy responsible for this induced grain size effect is confirmed from the high resolution micrographs taken close to the Cu/{Co/Cu} interface, as shown in Fig. 3(c). In the superlattice, both Cu and Co grow in the fcc form as expected,[10,19] maintaining epitaxy through the grain. Cu(111) planes (d=2.087 Å) extend directly from the underlayer grain into the multilayer. The Co layers can only be identified by very close inspection of the lattice fringes which are slightly distorted in those regions. The compositional layering showing individual Co and Cu layers is evident from Fig. 3(b). The layers in this case are continuous but wavy. Grain boundary grooving on the Cu underlayer surface causes the layers to bend in some locations. The inset to Fig. 3(c) shows a SAED pattern from this superlattice. The Co/Cu(111) ring again does not indicate any preferred orientation effects. In comparison with Fig. 2, it can be concluded that the diffraction patterns from both thin films are very similar implying that no orientational preferences can be distinguished. The primary difference between the two structures, as required, is their grain size.

Resistivity versus field data (for current orthogonal to field) are compared in Fig. 4 for two identical Co/Cu multilayers with Cu spacer layer thicknesses of 20 Å, grown with and without 350 Å Cu underlayers. This Cu layer thickness corresponds to the second MR peak. At both room temperature and 4.2 K the magnetoresistance of the structure grown on the Cu underlayer is larger but the difference is greater at lower temperatures. Note also that the resistance ratio [R(300 K)/R(4.2 K)] and the resistivity (at high field) of the Co/Cu multilayers is only weakly dependent (plus/minus about 4%) on the presence of the Cu underlayer although shunting by the Cu underlayer causes a drop in MR values as compared to multilayers studied previously.[9] Similar results are obtained independent of the Cu spacer thickness, for Cu layer thicknesses giving rise to antiferromagnetic coupling at the second peak, as shown in Fig. 5. Note that the thinnest Cu spacer thickness shown lies at the boundary between antiferromagnetic and ferromagnetic coupling and the coupling is not well defined.

The increased GMR for the Co/Cu multilayers with larger

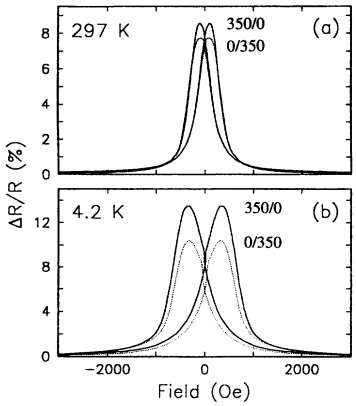

FIG. 4. Resistivity versus in-plane orthogonal field curves at (a) 297 K and (b) 4.2 K for Co/Cu multilayer samples (having Cu thickness of 20 Å) grown without underlayer (dotted line, referred to as 0/350) and with underlayer (solid line, referred to as 350/0).

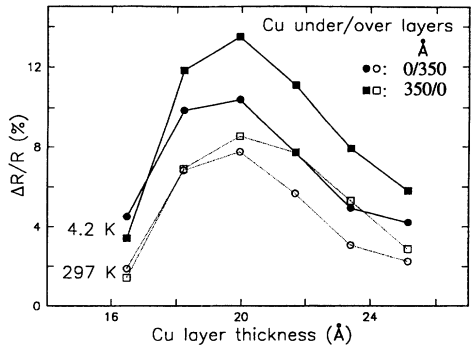

FIG. 5. Saturation magnetoresistance versus Cu spacer layer thickness at 297 K (open icons) and 4.2 K (closed icons) for two sets of Co/Cu multilayers grown without (circles) or with 350 Å underlayer (squares).

grain sizes cannot be accounted for by simple changes in the resistivity of the multilayers which, as mentioned earlier, are not substantially different. A straightforward hypothesis is that the increased grain size leads to a longer mean free path for electrons propagating across the Co and Cu layers in the structures. This would lead to sampling of a larger number of antiferromagnetically coupled Co layers in the large-grained multilayers as compared to the fine-grained multilayers. Consistent with this hypothesis is the weaker temperature dependence of GMR in the latter structures, where the sampling could be limited by the fine grain size. In the large-grained structures the sampling is likely to increase at low temperatures with increases in the relevant mean free path.

In summary, Co/Cu superlattices of different grain sizes were tailored by growing with and without a Cu underlayer. Grain-to-grain epitaxy caused the large grain underlayer structure to propagate into the multilayer in the former case, whereas the multilayer without any underlayer in the latter had a fine grain morphology. The room temperature magnetoresistance (MR) showed a slight increase whereas low temperature (Liquid He) MR showed a distinct increase with increasing grain size. The enhancement of MR with grain size, which should also apply to the first MR peak, can be related to an increase in the mean free path for electron scattering which leads to sampling of a larger number of antiferromagnetically coupled layers. This result should have general applicability to other sputter-deposited magnetic multilayers.

A.R.M. is pleased to acknowledge support from IBM and we thank K. P. Roche for technical support. The electron microscopy was carried out in the Center for High Resolution Electron Microscopy at Arizona State University supported by NSF Grant No. DMR-91-15680. This work was partially supported by the Office of Naval Research.

*Also at the Department of Physics, Arizona State University, Tempe, AZ 85287.

[1] S. S. P. Parkin *et al.*, Phys. Rev. Lett. **64**, 2304 (1990).
[2] A. Cebollada *et al.*, J. Magn. Magn. Mater. **102**, 25 (1992).
[3] S. S. P. Parkin *et al.*, Phys. Rev. Lett. **66**, 2152 (1991).
[4] S. S. P. Parkin, Phys. Rev. Lett. **67**, 3598 (1991).
[5] M. T. Johnson *et al.*, Phys. Rev. Lett. **68**, 2688 (1992).
[6] Z. Q. Qui *et al.*, Phys. Rev. B **46**, 8659 (1992).
[7] M. N. Baibich *et al.*, Phys. Rev. Lett. **61**, 2472 (1988).
[8] G. Binasch *et al.*, Phys. Rev. B **39**, 4828 (1989).
[9] S. S. P. Parkin *et al.*, Appl. Phys. Lett. **58**, 2710 (1991).
[10] S. S. P. Parkin *et al.*, Phys. Rev. B **47**, 9136 (1993).
[11] W. F. Egelhoff and M. T. Kief, Phys. Rev. B **45**, 7795 (1992).
[12] D. Grieg *et al.*, J. Magn. Magn. Mater. **110**, L239 (1992).
[13] J. Kohlepp *et al.*, J. Magn. Magn. Mater. **111**, L231 (1992).
[14] J. P. Renard *et al.*, J. Magn. Magn. Mater. **115**, L147 (1992).
[15] S. S. P. Parkin *et al.*, Phys. Rev. B **46**, 9262 (1992).
[16] G. R. Harp *et al.*, Phys. Rev. B **47**, 8721 (1993).
[17] P. Bruno and C. Chappert, Phys. Rev. Lett. **67**, 1602 (1991).
[18] J. Mathon, J. Magn. Magn. Mater. **100**, 527 (1991).
[19] A. R. Modak *et al.*, J. Magn. Magn. Mater. **129**, 415 (1994).
[20] K. L. Chopra, *Thin Film Phenomena* (McGraw Hill, New York, 1969).
[21] J. A. Thornton, Annu. Rev. Mater. Sci. **7**, 239 (1977).
[22] M. Ohring, *The Materials Science of Thin Films* (Academic, San Diego, 1991).
[23] D. E. Laughlin and B. Y. Wong, IEEE Trans. Magn. **27**, 4713 (1991).
[24] A. F. Mayadas *et al.*, J. Appl. Phys. **45**, 2780 (1974).
[25] T. I. McGuirre and R. I. Potter, IEEE Trans. Magn. **11**, 1018 (1975).
[26] A. F. Mayadas *et al.*, J. Vac. Sci. Technol. **6**, 690 (1969).
[27] H. J. Frost *et al.*, Acta Metall. Mater. **38**, 1455 (1990).
[28] D. M. Mattox, J. Vac. Sci. Technol. A **7**, 1105 (1989).
[29] J. Bravman and R. Sinclair, J. Electron Microsc. Tech. **1**, 53 (1984).
[30] A. R. Modak *et al.*, Ultramicroscopy **47**, 375 (1992).
[31] D. J. Smith *et al.*, Scripta Metall. Mater. **30**, 689 (1994).
[32] J. M. Cowley, *Diffraction Physics* (North Holland, New York, 1986).

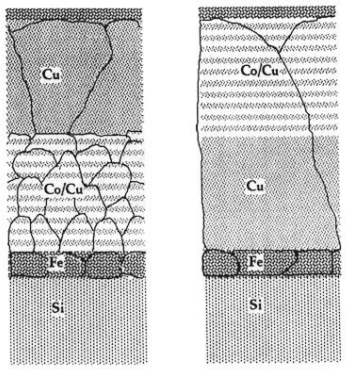

FIG. 1. Schematic illustration of proposed nominal multilayer structures and expected grain sizes.

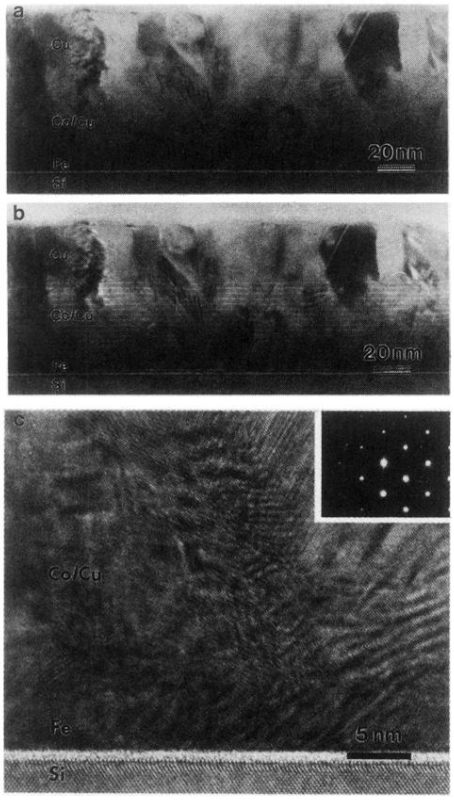

FIG. 2. (a) Bright-field transmission electron micrograph showing cross section of Co/Cu multilayer with nominal structure Si(100)/Fe(50 Å)/{Co(10 Å)/Cu(20 Å)}$_{15}$/Co(10 Å)/Cu(350 Å)/Fe(25 Å). (b) Image at large underfocus (~2000 Å) showing compositional layering. (c) High resolution electron micrograph showing characteristic fine grain structure. SAED pattern (inset) shows [110] oriented Si(100) spots and Co/Cu diffraction rings.

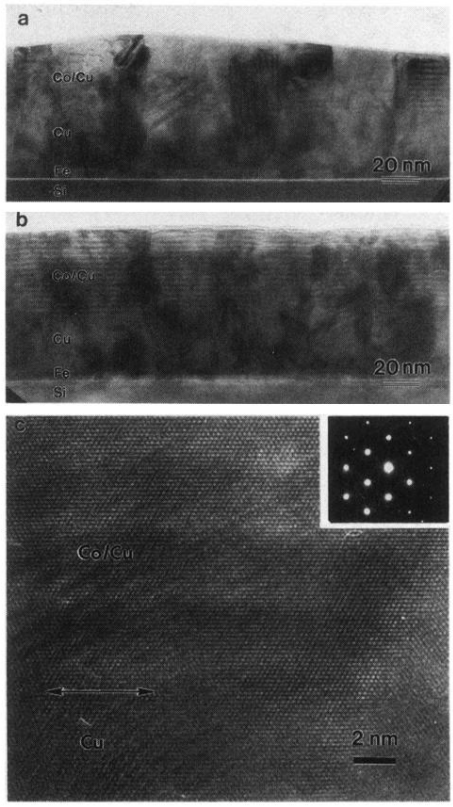

FIG. 3. (a) Bright field transmission electron micrographs showing cross section of Co/Cu multilayer with nominal structure Si(100)/Fe(50 Å)/Cu(350 Å)/{Co(10 Å)/Cu(20 Å}$_{15}$/Co(10 Å)/Fe(25 Å). (b) Image at large underfocus (~2000 Å) from same multilayer showing compositional layering. (c) High resolution electron micrograph showing grain-to-grain epitaxy at Cu/{Co/Cu} interface (marked by an arrow). Cu(111) planes are visible extending through Cu as well as {Co/Cu} superlattice.